HHS Public Access

Author manuscript

Neuropharmacology. Author manuscript; available in PMC 2019 April 29.

Published in final edited form as:

Neuropharmacology. 2018 August ; 138: 160–169. doi:10.1016/j.neuropharm.2018.06.009.

Osteopontin attenuates inflammation via JAK2/STAT1 pathway in hyperglycemic rats after intracerebral hemorrhage

Lei Gong[a,b,1], **Anatol Manaenko**[c], **Ruiming Fan**[d,1], **Lei Huang**[b], **Budbazar Enkhjargal**[b], **DevinW. McBride**[b], **Yan Ding**[b], **Jiping Tang**[b], **Xiaoqiu Xiao**[a,**], and **John H. Zhang**[b,*]

[a]Department of Obstetrics and Gynecology, The First Affiliated Hospital, Chongqing Medical University, Chongqing, 400016, China

[b]Department of Physiology and Pharmacology, School of Medicine, Loma Linda University, Loma Linda, CA, 92354, USA

[c]Departments of Neurology, University of Erlangen-Nuremberg, Erlangen, Germany

[d]Department of Cerebrovascular, The Affiliated Hospital, Zunyi Medical University, Guizhou, 563000, China

Abstract

Acute intracerebral hemorrhage (ICH) complicated by hyperglycemia is associated with aggravation of post-stroke inflammation, leading to exacerbation of brain edema and predicting poor neurological outcomes and higher mortality of patients. Osteopontin (OPN) is a neuroprotective glycoprotein, which is able to attenuate brain injury induced by hemorrhagic stroke. In the current study we investigated whether OPN will decrease the inflammatory post-ICH response as well as attenuate brain edema and neurological deficits in hyperglycemic rats. We employed a collagenase model of ICH on male Sprague-Dawley rats (n = 148) rats and 50% of Dextrose was injected intraperitoneally (i.p) 3 h after ICH (ICH + HG). Intranasal administration of recombinant OPN (rOPN) was performed 1 h after ICH. The development of brain injury was evaluated by brain water content (BWC) and neurological deficits, western blot and immunohistochemistry study. Small interfering ribonucleic acid (siRNA) for integrin-β1 receptor and a JAK2 agonist, Coumermycin A1 (C-A1), were used for detailed investigation of the molecular pathway. The administration of OPN (3 μg) significantly improved neurobehavior and increased expression of OPN and integrin-β1 receptor in the brain followed with decrease of neutrophil infiltration, JAK2, STAT1, TNF-a, IL-1b, MMP-9 and brain edema in the ICH + HG +

*Corresponding author. Departments of Anesthesiology and Physiology, Loma Linda University School of Medicine, 11041 Campus St, Risley Hall, Room 219, Loma Linda, CA, 92354, USA. **Corresponding author. Department of Obstetrics and Gynecology, the First Affiliated Hospital, Chongqing Medical University, Chongqing, 400016, China.

[1]The first two authors contributed equally to this work.

Author contribution statement

The idea and design were made by Lei Gong, John H Zhang, Jiping Tang and Xiaoqiu Xiao. Drafting the article was done by Lei Gong, Anatol Manaenko and Ruiming Fan. Lei Gong and Ruiming Fan performed most experiments. Critically revising the article was made by all authors. Reviewed submitted version of manuscript was made by all authors. John H Zhang and Xiaoqiu Xiao approved the final version of the manuscript on behalf of all the authors.

Disclosures/Conflict of interest

The author(s) declared no potential conflicts of interest with respect to the research, authorship, and/or publication of this article.

Appendix A. Supplementary data

Supplementary data related to this article can be found at https://doi.org/10.1016/j.neuropharm.2018.06.009.

OPN rats compared with ICH + HG rats. The effects of OPN were reversed by the intervention of intergrin-β1 siRNA and C-A1. In conclusion, rOPN attenuated ICH-induced brain inflammation in hyperglycemic rats, leading to attenuation of brain edema and improving neurological functions. Effects of rOPN were mediated at least partly by integrin-β1 induced inhibition of JAK2/STAT1 pathway.

Keywords

ICH; Hyperglycemia; Osteopontin; Inflammation; Brain edema

1. Introduction

Brain inflammation is a major pathophysiological factor, which significantly contributes to the development of secondary brain injury and consequently to high mortality and morbidity of patients after intracerebral hemorrhage (ICH). Shortly after ICH, activated microglia increased production of such inflammatory mediators as TNF-α (Rendevski et al., 2017; Wang et al., 2003). TNF-α can directly disturb function of the bloodebrain barrier (BBB) allowing the blood elements to infiltrate the brain, aggravating the brain inflammation after ICH (Kawanishi et al., 2008; Lv et al., 2010). The cumulative inflammatory effects induced by microglia, toxic elements of blood degradation and immune cells, infiltrated brain, results in development of brain injury and neurological dysfunctions after ICH. Therapeutic strategies, which are able to attenuated post-ICH inflammation, are promising approaches, which can decrease mortality and morbidity of ICH patients (Omoyinmi et al., 2017).

Osteopontin (OPN) is an inducible pleiotropic extracellular matrix glycoprotein, which physiologically interacts with several subforms of integrin-β1 (Uede, 2011). Upon this interaction OPN regulates development of numerous diseases, between others OPN attenuates development of secondary brain injury after hemorrhagic stroke (Suzuki et al., 2010; Wu et al., 2016). However, a role of OPN on the neuroinflammation has never been studied previously in ICH. In this study, we aimed to investigate whether intranasally administrated recombinant osteopotin (rOPN) will attenuate inflammation and infiltration of neutrophils, resulting in attenuation of perihematomal edema formation in the brain and consequently improving neurologic functions of hyperglycemic rats after ICH. Furthermore, we explored molecular mechanisms underlying OPN induced protection.

2. Materials and methods

2.1. Animals

All experimental procedures were performed following a corresponding study protocol approved by the Institutional Animal Care and Use Committee (IACUC) of Loma Linda University in accordance with the NIH Guide for the Care and Use of Laboratory Animals. A total of 148 adult male Sprague-Dawley rats (weight 280–320 g, Charles River, Wilmington, MA) housed in a light and temperature controlled room with sufficient food and water were used in this study.

2.2. Experimental design

To determine expression of the key protein related to integrin-β1 dependent mechanism in hyperglycemic rats after ICH (ICH + HG), 47 rats were randomly assigned into 6 groups in time course experiments: sham (n = 6) and ICH + HG at 6, 12, 24, 48, 72 h after ICH induction. 50% Dextrose (8 ml/kg, Hospira, Inc.) was injected intraperitoneally (i.p) 3 h after ICH. Western blots were used to detect the protein expression of integrin-β1, OPN, p-JAK2, JAK2, p-STAT1 and STAT1 in the right hemisphere of the brain. Cellular localization of integrin-β1 in microglia and astrocytes was detected with immunohistochemistry (IHC) staining after 24 h after in sham and ICH + HG groups (n = 3 per group).

Next, to evaluate the effect of rOPN after ICH + HG, 53 rats were randomly divided into 8 groups at 24 h and 72 h after ICH induction. For 24 h, there are five subgroups: sham (n = 6), ICH + HG + vehicle (30 μL of sterile 0.9% NaCl; n = 7), ICH + HG + rOPN 1 μg (1 μg in 30 μL of sterile 0.9% NaCl; n = 6), ICH + HG + rOPN 3 μg (3 μg in 30 μL of sterile 0.9% NaCl; n = 7), ICH + HG + rOPN 9 μg (9 μg in 30 μL of sterile 0.9% NaCl; n = 6). For 72 h, there are three subgroups: sham (n = 6), ICH + HG + vehicle (n = 8), and ICH + HG + rOPN 3 μg (n = 7). Neurological scores and brain water content were assessed respectively at 24 h and 72 h after ICH.

Finally, to determine molecular mechanism, 48 rats were randomly assigned into 5 groups: ICH + HG + vehicle (n = 10), ICH + HG + Integrin-β1 siRNA (n = 9), ICH + HG + Scramble siRNA (n = 9), ICH + HG + rOPN (n = 9), ICH + HG + rOPN + Coumermycin A1 (C-A1) (100 μg/kg, Santa Cruz) (n = 11). C-A1, a JAK2 agonist, and sterile 0.9% NaCl were administered i.p 1 h after ICH induction. Western blots and MPO staining were performed 24 h after ICH in all groups.

2.3. Animal model and experimental protocol

One hundred and forty-eight, 8-week-old male SD rats (weight 280–320 g, Charles River, Wilmington, MA) were used. ICH rats model was performed by collagenase injection as reported previously (Manaenko et al., 2018). 50% Dextrose was injected intraperitoneally (i.p) 3 h after ICH to induce acute hematoma expansion (Zheng et al., 2015).

2.4. Blood glucose measurement

The level of blood glucose was monitored within 24 h after injecting i.p 50% Dextrose. To this end, the tail vein was punctured and 10 μL of blood was collected. The glucose level was measured using hemoglucometer (Aim Strip Plus Blood Glucose Meter Germanine Laboratories, INC.) Inclusion criteria require a blood glucose level of 175 mg/dl to 300 mg/dl within 24 h after injecting i.p 50% Dextrose.

2.5. Measurement of hemorrhagic volume (hemoglobin assay)

The spectrophotometric hemoglobin assay was performed as described before (Lekic et al., 2013). Extracted brainstem tissue was placed in glass test tubes with 3 ml of PBS and then homogenized for 60 s (Tissue Miser Homogenizer, Fisher Scientific). Ultrasonication for 1 min lysed erythrocyte membranes, the products were centrifuged for 30 min, and Drabkin reagent was added (Sigma-Aldrich) into aliquots of supernatant fluid that reacted for 15 min.

Absorbance, using a spectrophotometer (540 nm; Genesis 10uv, Thermo Fisher Scientific), was calculated into a hemorrhagic volume on the basis of a standard curve.

2.6. Brain water content (BWC) measurement

Brain water content was measured as previously described (Yang et al., 2016). Briefly, mice were decapitated under deep anesthesia. Brains were immediately removed and cut into 4 mm sections around the needle track. Each section was divided into four parts: ipsilateral and contralateral basal ganglia, ipsilateral and contralateral cortex. The cerebellum was collected as an internal control. Each part was weighed on an electronic analytical balance (APX-60, Denver Instrument) and then dried at 100 °C for 24 h to determine the dry weight (DW). Brain water content (%) was calculated as [(WW – DW)/WW] × 100.

2.7. Nasal administration of rOPN

Intranasal administration of rOPN was performed 1 h after ICH-induction. Under isoflurane anesthesia, were placed in a supine position and 0.9% NaCl or rOPN dissolved in sterile 0.9% NaCl was administered alternately into the left and right nares, one drop every 2 min over a period of 12 min (Xie et al., 2017). A total volume of 30 μL was administered. Three different dose of rOPN were tested (1 μg, 3 μg, 9 μg).

2.8. Intracerebroventricular injection

Intracerebroventricular (i.c.v) drug administration was performed as reported previously (Ma et al., 2017; Tong et al., 2017). Briefly, rats were positioned prone in a stereotaxic apparatus under 2.5% isoflurane anesthesia. A burr hole was drilled into the skull according to the following coordinates relative to bregma: 0.92 mm posterior and 1.5 mm lateral. The needle of a 10 μL Hamilton syringe (Microliter 701; Hamilton Company, Reno, NV) was inserted into the left lateral ventricle through the burr hole 3.3 mm below the horizontal plane of bregma. Integrin β1 siRNA (10 μM/10 μL, Santa Cruz, USA) or scrambled siRNA (10 μM/10 μL, Santa Cruz, USA) was infused at the same rate 48 h before ICH induction.

2.9. Neurological scores

Twenty-four or 72 h after ICH, the Garcia test was performed by a blinded investigator as previously described with modifications (Manaenko et al., 2011). The scores given to each of the rats at the completion of the evaluation was the summation of 7 individual test scores (spontaneous activity, symmetry in the movement of four limbs, forepaw outstretching, climbing, body proprioception, response to vibrissae touch, and beam walking). The neurological scoring ranged from 2 (most severe deficit) to 21 (maximum).

2.10. Immunohistochemistry staining

The brain tissues were collected at 24 h after ICH. Immunofluorescent staining for brain samples was performed on fixed frozen ultrathin sections as previously described (Zheng et al., 2015). Primary antibodies used were anti-Integrin-β1 primary antibody (1:200, ab179471, MA, USA), anti-MPO (sc-16128, 1:200, Santa Cruz Biotechnology), anti-GFAP (1:500, ab110062), and anti-Iba-1 (1:100, ab107159). Peri-hemorrhagic area of the brain coronal section was imaged by Leica DMi8 (Leica microsystems, Germany).

2.11. Western blot analysis

24 h after surgery, the rats under deep anesthesia were perfused via intracardially with 150 ml of ice cold PBS and brain samples were collected. Protein extraction and Western blots were performed according to the manufacturer's recommendation, as previously reported (Manaenko et al., 2011). Whole-cell lysates were obtained by gently homogenizing in RIPA lysis buffer (Santa Cruz Biotechnology, Inc., sc-24948) and centrifuging (14,000 g at 4 °C for 30 min). The supernatant of the extract was collected, and the protein expression was determined using a detergent compatible assay (Bio-Rad, Dc protein assay). Equal amounts of protein (50 μg) were loaded and subjected to electrophoresis on an SDS-PAGE gel. After being electrophoresed and transferred to a nitrocellulose membrane, the membrane was blocked and incubated with the primary antibody overnight at 4 °C. For an internal control, the same membrane was probed with an antibody against β-actin after being stripped. Secondary antibodies (Santa Cruz Biotechnology) were incubated for 1 h at room temperature. Immunoblots were then probed with an ECL Plus chemiluminescence reagent kit (Amersham Biosciences, Arlington Heights, IL) and visualized with an imaging system (Bio-Rad, Versa Doc, model 4000). Data was analyzed using Image J software. Following primary antibodies used were: OPN (1:1000, sc-21742, Santa Cruz Biotechnology), integrin-β1 (1:1000, ab179471, MA, USA), pJAK2/JAK2 (1:1000, ab32101/ab39636, MA, USA), pSTAT1/STAT1 (1:1000, ab30645/ ab31369, MA, USA), IL-1β (1:1000, ab9722, MA, USA), TNF-α (1:1000, ab6671, MA, USA), MMP-9 (1:500, ab38898, MA, USA), MPO (1:500, sc-16128, Santa Cruz Biotechnology), and β-actin (1:3000, I-19, Santa Cruz Biotechnology, CA).

2.12. Statistical analysis

The analysis of the data was performed using GraphPad Prism and SPSS 22.0 software. Statistical differences between two groups were analyzed using the student's unpaired, two-tailed t-test. Multiple comparisons (without a rating scale) were statistically analyzed with one-way analysis of variance (ANOVA) followed by the Tukey method. Mortality was statistically analyzed with Chi-square test. The data are presented as mean ± SEM. In all statistical analysis, a value of $P < 0.05$ represents statistical significance.

3. Results

3.1. Mortality

Of the 148 total animals, 21 rats were subjected to sham and 127 rats were subjected to ICH + HG induction, with total 10 (8%) animals died within 24 h and total 3 (14%) animals died at 72 h after surgery. The animals were divided randomly in each groups. The mortality within 24 h after surgery in this study was as follows in each group: sham, 0% (0 died of 9 rats in time course study); ICH, 13% (5 died of 38 rats in time course study); sham, 0% (0 died of 6); ICH + HG + vehicle,12% (2 died of 17); ICH + HG + rOPN, 4% (1 died of 28); ICH + HG + Scramble siRNA, 0% (0 died of 9); ICH + HG + Integrin-β1 siRNA, 0% (0 died of 9); ICH + HG + rOPN + Coumermycin,18% (2 died of 11). The mortality at 72 h after surgery in this study was as follows in each group: sham, 0% (0 died of 6); ICH + HG + vehicle, 25% (2 died of 8); ICH + HG + rOPN, 14% (1 died of 7). (Table 1).

3.2. Ip injection of glucose resulted in increased blood glucose level

Blood glucose peaked 1 h after intraperitoneal injection of 50% dextrose, and returned to the baseline within 4 h, and rOPN had no effect on blood glucose level (Supplemental Fig. 1).

3.3. Effects of ICH + HG on the expression of OPN and integrin-β1/JAK2/STAT1 pathway's proteins

The endogenous expression of OPN was no changes in earlier stages of ICH compared to sham group. At 24 h we observed significant decrease of OPN followed by significantly upregulation of the production at 48 h. The production remained upregulated at 72 h after ICH (Fig. 1A and B). Similar pattern of expression changes were observed by the integrin-β1. The expression of integrin-β1 was significantly decreased at 24 h and up-regulated at 48 and 72 h after ICH (Fig. 1 A and C). Additionally, ratio of p-JAK2 and p-STAT1 to total JAK2 and STAT1, respectively, were significantly increased at 24 h after ICH (Fig. 1 A, D and E). Furthermore, colocalization of integrin-β1 with microglia (Iba-1) and astrocytes (GFAP) was observed in the perihematoma area of ipsilateral hemisphere after 24 h after ICH induction (Fig. 2).

3.4. Effects of rOPN intranasal administration on the brain injury after ICH

ICH resulted in significant increase of brain water content in the ipsilateral basal ganglia 24 h after ICH (Fig. 3 A). Consequently significant neurological dysfunctions were observed in all ICH compared to sham operated animals (Fig. 3B–C). While low dose of OPN was ineffective, but both medium and high doses of OPN significantly decreased ICH-induced brain water content elevation, leading to improvement of neurological functions evaluated by modified Garcia and beam balance tests (Fig. 3A–C). No significant difference in effects of high and medium doses of OPN was observed. Therefore the medium dose was used to investigate time dependent effects of OPN in further experiments. Compared to sham operated animals the increased brain water content was detected both in ipsilateral basal ganglia and in cortex as evaluated at 72 h after ICH (Fig. 3 D). OPN attenuated the increase of brain water content, resulting in amelioration of ICH-induced neurological dysfunctions (Fig. 3B and C, E and F).

3.5. Effects of rOPN on the JAK2/STAT1 pathway and neutrophil infiltration

Intranasal administration of rOPN dose-dependently increased OPN expression in brain. While low dose of rOPN (1 μg) had no effect on endogenous OPN expression, medium (3 μg) and high (9 μg) doses of rOPN increased brain OPN expression above level, which was observed in sham operated animals. No difference between medium and high doses of rOPN was observed (Fig. 4 A). The increase of OPN amount in brain was accompanied with an accumulation of integrin-β1 (Fig. 4 B). ICH induced an increase ration of phosphorylated/total JAK2 and STAT1. The OPN increase was accompanied with the decrease of phosphorylated to total protein ratio of both JAK2 and STAT1 (Fig. 4C and D, respectively). Moreover, ICH induced overproduction of TNF-α and Il-1β, which was accompanied with MMP-9 activation (Fig. 4E–G). rOPN induced inhibition of JAK2/STAT1 pathway resulted in the decrease of TNF-α and Il-1β production (Fig. 4E–F), which in turn led to dose dependent decrease the ICH-induced overexpression of MMP-9 (Fig. 4 G). Furthermore,

rOPN administration attenuated post-ICH brain infiltration by neutrophils, evaluated by immunostaining and western blot to neutrophils specific protein, MPO (Fig. 5A–C).

3.6. Integrin-β1 siRNA and JAK2 agonist reversed the effect of rOPN

While scramble siRNA shown no effect, siRNA induced in-vivo knock down of integrin-β1 resulted in significant down regulation of the integrin-β1 leading to the increase of phosphorylated to total protein ratio of JAK2 and STAT1 (Fig. 6A–C) and aggravating the brain inflammation (Fig. 6D–E) and activating MMP-9 (Fig. 6 F) and to more brain infiltration by neutrophils (representative immunostaining Fig. 7A, evaluation of neutrophils infiltration by western blot Fig. 7A–C). As expected, an activation of JAK2 by C-A1 had no effect on integrin-β1 expression, however, compared to OPN treated animals, increased ratio of phosphorylated JAK2 to total JAK2, resulting in the increase of ratio of phosphorylated STAT1 to total STAT1. That reversed effects of OPN and increased expression of Il-1β, TNF-α and MMP-9 in post ICH brain (Fig. 6) as well as increased the brain infiltration by neutrophils (Fig. 7) in ICH + HG rats.

4. Discussion

In this study we demonstrated that intranasally administrated rOPN attenuated the development of secondary brain injury in hyperglycemic rats after ICH. We demonstrated furthermore that protective effects of rOPN are mediated, at least partly, by integrin-β1, which was able to attenuated ICH induced activation of JAK2/STAT1 pathway, decreasing post-ICH inflammation.

The acute hyperglycemia is common for the patients with preexisting diabetes. After ICH, however, more than 59% of patients without diabetes show increase blood glucose concentration on admission, and blood glucose level remains upregulated till 72 h after admission in 45% of patients (Bejot et al., 2012; Godoy et al., 2008; Wu et al., 2017). The high level of glucose is a predisposition for worth neurological outcomes, poor functional recovery at discharge and increased 1-month mortality after ICH (Bejot et al., 2012; Godoy et al., 2008). In preclinical studies, the combination stroke/hyperglycemia induces bigger hematoma, higher level of inflammation and apoptosis, consequently leading to the aggravation of post-ICH brain injury and neurological dysfunctions (Chiu et al., 2012; Zheng et al., 2015). The hyperglycemia in animals can be induced by intraperitoneal injection of glucose as we did in current study and before (Zheng et al., 2015).

We established that ICH increased the endogenous OPN production starting at 48 h after ICH + HG. That was in agreement with previous publication, demonstrating increase of endogenous OPN production after hemorrhagic stroke in animals and human patients (Nakatsuka et al., 2018; Suzuki et al., 2010). We hypothesized that the endogenous OPN is able to decrease brain injury and the increase of OPN production is a protective stress reaction of the brain. That is in agreement with presvious publication, demonstrating that pre-treatment via intracerebroventricular infusion of rOPN 20 min pre-ICH attenuates development of brain edema and improves neurological functions of mice (Wu et al., 2011). We demonstrated previously that the development of brain edema after experimental ICH is time dependent and reach maximum 24/72 h after ICH (Manaenko et al., 2011). Free iron

accumulation and iron induced oxidative stress peaks at 72 h after ICH (Xi et al., 2006). Since at this time point the OPN expression peaks, we hypothesized that OPN production increases parallel with the development of brain injury and that earlier increase of OPN expression in brain will prevent the development of brain injury. In order to investigate the potential mechanism of OPN we monitored the expression of integrin-β1 as well as the expression of JAK2 and STAT1. We established that integrin-β1 is expressed in Iba-1and GFAP positive cells and that ICH induced OPN overproduction was associated with integrin-β1 overproduction at 48–72 h after ICH. That is in agreement with previous findings demonstrating that overproduction of OPN was accompanied with the increased integrin-β1 production (Zou et al., 2013). Furthermore, it is known that integrin-β1 effects are mediated, at least partly, by its ability to inhibit JAK/STAT pathway (Yan et al., 2017). To study whether this pathway is relevant in our particular model we first investigated effects of ICH on JAK/STAT expression and activation. While some studies demonstrated that stroke induced activation via phosphorylation of this proteins there are publications demonstrating that stroke can increase the expression of the proteins as well (Justicia et al., 2000; Spudich et al., 2005). In agreement with these studies we demonstrated that ICH significantly increased both expression and phosphorylation of the STAT1. Similar results, demonstrating that rOPN is able to attenuate ICH induced STAT1 phosphorylation was demonstrated before (Wu et al., 2011). Additionally, we observed that the JAK2/STAT1 pathway was activated at time point, on which no up-regulation of integrin-β1 was observed. The increase of integrin-β1 expression was associated with inhibition of JAK/STAT pathway.

In the next experiment we investigated effects of intranasal administration of recombinant OPN on the development of secondary brain injury and neurological dysfunctions after ICH. The maximal molecular weight of a substance, which can penetrate intact BBB varies, according to different study, from 0.4 till 7.8 kDa (Banks, 2009). The molecular weight of OPN is 33 kDa, such molecular weight it will not allow rOPN to penetrate BBB. For this reason we have chosen the intranasal route of drug administration. The intranasal administration is a safe, none invasive and reliable way of high molecular weight drug delivery over the intact BBB. This way of drug administration provides a direct route to the brain. After administration a drug will undergo endocytosis and be transported along olfactory nerves or by extracellular flow through intercellular clefts in the olfactory epithelium and to diffuse into the subarachnoid space (Thorne et al.,1995). The efficiency of this route of drug administration in pre-experimental animal models was demonstrated before (Wu et al., 2016). In current study we established that intranasal administration dose dependently increased amount of rOPN in the brain. The maximal increase of OPN amount in the brain was achieved with medium and high dose of the drug. The OPN increase, induced by medium and high OPN dose, was accompanied with amelioration of peri-hematomal brain edema development in ICH treated compared to none-treated animals. The development of brain edema was evaluated by brain water content calculation (Manaenko et al., 2018). The decrease of brain water content confirmed our working hypothesis, that OPN is able to decrease inflammation and stabilize BBB after ICH. The decrease of brain water content resulted in significant improvement of neurological functions (Manaenko et al.,

2011). Furthermore the improved functions of BBB led to the attenuation of brain infiltration by MPO positive neutrophils.

This results contradict previous funding demonstrating that high OPN is an independent predictor for poor outcome after another kind of hemoragic stroke, a subarachnoid hemorrhage in human patients (Nakatsuka et al., 2018). It is however worth to mention that authors of this publication measured OPN concentration in plasma. As mentioned before OPN, due to high molecular weight, does not pass BBB and the plasma concentration of the substance does not mirror changes in brain concentration. The patients with high OPN had more prominent neurological dysfunction. With presented data is difficult to understand is a systemic overproduction of OPN a response of organism on more severe brain damage or systemic produced OPN contributes to the development of brain injury after SAH. Furthermore authors determinated that high OPN in blood correlates with development of vasospasm and consequently with delayed cerebral infarction. It is theoretically possible that systemic OPN induced vasospasm and on this way damages post-SAH brain without penetrating BBB. However arise of vasospasm after ICH in unknown and it is unlikely that systemic OPN can induce additionally brain damage after ICH as well. Having said that we admit that the results presented by Nakatsuka et al. clearly indicated that role of OPN in development of brain injury after stroke is not fully understood. Futher investigation, especially of role of OPN on the development of long term brain injury and neurological disfunctions are uregently needed.

To investigate the molecular pathway underlying observed beneficial effects of rOPN, we proved whether OPN is able to affect the integrin-β1 expression and consequently to inhibit JAK2/STAT pathway. While low dose of rOPN had no effect on integrin-β1 expression, medium and high dose of rOPN significantly increased expression of integrin-β1 and inhibited JAK2/STAT1 pathway. It has been demonstrated that JAK/STAT pathway modulates inflammatory response after stroke (Hou et al., 2010; Tao et al., 2015; Wasserman et al., 2007; Zhou et al., 2014). In agreement with these we observed that rOPN induced inhibition of JAK/STAT pathway significantly attenuated post- ICH overproduction of TGF-α and IL-1β. The decrease of inflammatory marker production was, furthermore, associated with less MMP-9 expression and significant attenuated brain infiltration by neutrophils.

To further strong our working hypothesis we induced in vivo knock down of integrin-β1 via i.c.v administration of siRNA. These administration route of siRNA proofed itself as a reliable way for induction of in vivo knock down (Manaenko et al., 2018). While scramble RNA had not effect on integrin-β1, siRNA induced knock down resulted in significant downregulation of integrin-β1 expression. Knock down of integrin-β1 resulted in turn in activation of JAK2/STAT1 and increased production of IL-1β and MMP-9 as well as aggravated brain inflammation by neurophils.

So far we established that rOPN effects are mediated through JAK2/STAT1 pathway. In the last experiment we examined if activation of JAK2 is able to reverse rOPN effects. To activate JAK2 we employed C-A1, a compound able to induce JAK2 autophosphorylation (Mizuguchi and Hatakeyama,1998). Well in agreement with that we observed that C-A1 induced significant increase of phosphorylated/total JAK2 level, which in turn resulted in

activation of STAT2. No effects of C-A1 on integrin-β1 expression, confirming that integrin-β1 is an upstream of JAK2.

Furthermore we demonstrated that C-A1 induced activation of JAK2 reversed beneficial effects of rOPN and increased both production of pro-inflammatory factors and brain infiltration by neutrophils.

In conclusion, rOPN attenuated ICH-induced brain inflammation in hyperglycemic rats, leading to attenuation of brain edema, and improving neurological functions. Effect of rOPN were mediated at least partly by integrin-β1 and integrin-β1 induced inhibition of JAK2/STAT1 pathway.

Supplementary Material

Refer to Web version on PubMed Central for supplementary material.

Acknowledgements

This study is partially supported by NIH grants NS078755 and NS103822 to JHZ.

References

Banks WA, 2009 Characteristics of compounds that cross the blood-brain barrier. BMC Neurol. 9 (Suppl. 1), S3. [PubMed: 19534732]

Bejot Y, Aboa-Eboule C, Hervieu M, Jacquin A, Osseby GV, Rouaud O, Giroud M, 2012 The deleterious effect of admission hyperglycemia on survival and functional outcome in patients with intracerebral hemorrhage. Stroke 43, 243–245. [PubMed: 21940959]

Chiu CD, Chen TY, Chin LT, Shen CC, Huo J, Ma SY, Chen HM, Chu CH, 2012 Investigation of the effect of hyperglycemia on intracerebral hemorrhage by proteomic approaches. Proteomics 12, 113–123. [PubMed: 22065606]

Godoy DA, Pinero GR, Svampa S, Papa F, Di Napoli M, 2008 Hyperglycemia and short-term outcome in patients with spontaneous intracerebral hemorrhage. Neurocritical Care 9, 217–229. [PubMed: 18300001]

Hou YC, Liou KT, Chern CM, Wang YH, Liao JF, Chang S, Chou YH, Shen YC, 2010 Preventive effect of silymarin in cerebral ischemia-reperfusion-induced brain injury in rats possibly through impairing NF-kappaB and STAT-1 activation. Phytomedicine 17, 963–973. [PubMed: 20833521]

Justicia C, Gabriel C, Planas AM, 2000 Activation of the JAK/STAT pathway following transient focal cerebral ischemia: signaling through Jak1 and Stat3 in astrocytes. Glia 30, 253–270. [PubMed: 10756075]

Kawanishi M, Kawai N, Nakamura T, Luo C, Tamiya T, Nagao S, 2008 Effect of delayed mild brain hypothermia on edema formation after intracerebral hemorrhage in rats. J. Stroke Cerebrovasc. Dis 17, 187–195. [PubMed: 18589338]

Lekic T, Rolland W, Manaenko A, Krafft PR, Kamper JE, Suzuki H, Hartman RE, Tang J, Zhang JH, 2013 Evaluation of the hematoma consequences, neurobehavioral profiles, and histopathology in a rat model of pontine hemorrhage. J. Neurosurg 118, 465–477. [PubMed: 23198805]

Lv S, Song HL, Zhou Y, Li LX, Cui W, Wang W, Liu P, 2010 Tumour necrosis factor-alpha affects blood-brain barrier permeability and tight junction-associated occludin in acute liver failure. Liver Int. 30, 1198–1210. [PubMed: 20492508]

Ma L, Manaenko A, Ou YB, Shao AW, Yang SX, Zhang JH, 2017 Bosutinib attenuates inflammation via inhibiting salt-inducible kinases in experimental model of intracerebral hemorrhage on mice. Stroke 48, 3108–3116. [PubMed: 29018127]

Manaenko A, Fathali N, Khatibi NH, Lekic T, Hasegawa Y, Martin R, Tang J, Zhang JH, 2011 Arginine-vasopressin V1a receptor inhibition improves neurologic outcomes following an intracerebral hemorrhagic brain injury. Neurochem. Int 58, 542–548. [PubMed: 21256175]

Manaenko A, Yang P, Nowrangi D, Budbazar E, Hartman RE, Obenaus A, Pearce WJ, Zhang JH, Tang J, 2018 Inhibition of stress fiber formation preserves blood-brain barrier after intracerebral hemorrhage in mice. J. Cereb. Blood Flow Metab 38 (1), 87–102. [PubMed: 27864464]

Mizuguchi R, Hatakeyama M, 1998 Conditional activation of Janus kinase (JAK) confers factor independence upon interleukin-3-dependent cells. Essential role of Ras in JAK-triggered mitogenesis. J. Biol. Chem 273, 32297–32303. [PubMed: 9822709]

Nakatsuka Y, Shiba M, Nishikawa H, Terashima M, Kawakita F, Fujimoto M, Suzuki H, pSEED group, 2018 Acute-phase plasma osteopontin as an independent predictor for poor outcome after aneurysmal subarachnoid hemorrhage. Mol. Neurobiol

Omoyinmi E, Standing A, Keylock A, Price-Kuehne F, Melo Gomes S, Rowczenio D, Nanthapisal S, Cullup T, Nyanhete R, Ashton E, Murphy C, Clarke M, Ahlfors H, Jenkins L, Gilmour K, Eleftheriou D, Lachmann HJ, Hawkins PN, Klein N, Brogan PA, 2017 Clinical impact of a targeted next-generation sequencing gene panel for autoinflammation and vasculitis. PLoS One 12, e0181874. [PubMed: 28750028]

Rendevski V, Aleksovski B, Stojanov D, Mihajlovska-Rendevska A, Aleksovski V, Baneva-Dolnenec N, Nikodijevic D, Gudeva-Nikovska D, 2017 Validation of the ELISA method for quantitative detection of TNF-alpha in patients with intracerebral hemorrhage. Open Access Maced J. Med. Sci 5, 703–707. [PubMed: 29104676]

Spudich A, Frigg R, Kilic E, Kilic U, Oesch B, Raeber A, Bassetti CL, Hermann DM, 2005 Aggravation of ischemic brain injury by prion protein deficiency: role of ERK-1/−2 and STAT-1. Neurobiol. Dis 20, 442–449. [PubMed: 15893468]

Suzuki H, Hasegawa Y, Kanamaru K, Zhang JH, 2010 Mechanisms of osteopontin-induced stabilization of blood-brain barrier disruption after subarachnoid hemorrhage in rats. Stroke 41, 1783–1790. [PubMed: 20616319]

Tao Z, Cheng M, Wang SC, Lv W, Hu HQ, Li CF, Cao BZ, 2015 JAK2/STAT3 pathway mediating inflammatory responses in heatstroke-induced rats. Int. J. Clin. Exp. Pathol 8, 6732–6739. [PubMed: 26261556]

Thorne RG, Emory CR, Ala TA, Frey WH 2nd, 1995 Quantitative analysis of the olfactory pathway for drug delivery to the brain. Brain Res. 692, 278–282. [PubMed: 8548316]

Tong LS, Shao AW, Ou YB, Guo ZN, Manaenko A, Dixon BJ, Tang J, Lou M, Zhang JH, 2017 Recombinant Gas6 augments Axl and facilitates immune restoration in an intracerebral hemorrhage mouse model. J. Cereb. Blood Flow Metab 37, 1971–1981. [PubMed: 27389179]

Uede T, 2011 Osteopontin, intrinsic tissue regulator of intractable inflammatory diseases. Pathol. Int 61, 265–280. [PubMed: 21501293]

Wang J, Rogove AD, Tsirka AE, Tsirka SE, 2003 Protective role of tuftsin fragment 1–3 in an animal model of intracerebral hemorrhage. Ann. Neurol 54, 655–664. [PubMed: 14595655]

Wasserman JK, Zhu X, Schlichter LC, 2007 Evolution of the inflammatory response in the brain following intracerebral hemorrhage and effects of delayed minocycline treatment. Brain Res. 1180, 140–154. [PubMed: 17919462]

Wu B, Ma Q, Suzuki H, Chen C, Liu W, Tang J, Zhang J, 2011 Recombinant osteopontin attenuates brain injury after intracerebral hemorrhage in mice. Neurocritical Care 14, 109–117. [PubMed: 20440599]

Wu J, Zhang Y, Yang P, Enkhjargal B, Manaenko A, Tang J, Pearce WJ, Hartman R, Obenaus A, Chen G, Zhang JH, 2016 Recombinant osteopontin stabilizes smooth muscle cell phenotype via integrin receptor/integrin-linked kinase/rac-1 pathway after subarachnoid hemorrhage in rats. Stroke 47, 1319–1327. [PubMed: 27006454]

Wu TY, Putaala J, Sharma G, Strbian D, Tatlisumak T, Davis SM, Meretoja A, 2017 Persistent hyperglycemia is associated with increased mortality after intracerebral hemorrhage. J. Am. Heart Assoc 6.

Xi G, Keep RF, Hoff JT, 2006 Mechanisms of brain injury after intracerebral haemorrhage. Lancet Neurol. 5, 53–63. [PubMed: 16361023]

Xie Z, Huang L, Enkhjargal B, Reis C, Wan W, Tang J, Cheng Y, Zhang JH, 2017 Intranasal administration of recombinant Netrin-1 attenuates neuronal apoptosis by activating DCC/APPL-1/AKT signaling pathway after subarachnoid hemorrhage in rats. Neuropharmacology 119, 123–133. [PubMed: 28347836]

Yan Q, Jiang L, Liu M, Yu D, Zhang Y, Li Y, Fang S, Li Y, Zhu YH, Yuan Y, Guan XY, 2017 ANGPTL1 interacts with integrin alpha1beta1 to suppress HCC angiogenesis and metastasis by inhibiting JAK2/STAT3 signaling. Cancer Res.

Yang P, Manaenko A, Xu F, Miao L, Wang G, Hu X, Guo ZN, Hu Q, Hartman RE, Pearce WJ, Obenaus A, Zhang JH, Chen G, Tang J, 2016 Role of PDGF-D and PDGFR-beta in neuroinflammation in experimental ICH mice model. Exp. Neurol 283, 157–164. [PubMed: 27302678]

Zheng Y, Hu Q, Manaenko A, Zhang Y, Peng Y, Xu L, Tang J, Tang J, Zhang JH, 2015 17beta-Estradiol attenuates hematoma expansion through estrogen receptor alpha/silent information regulator 1/nuclear factor-kappa b pathway in hyperglycemic intracerebral hemorrhage mice. Stroke 46, 485–491. [PubMed: 25523052]

Zhou QB, Jin YL, Jia Q, Zhang Y, Li LY, Liu P, Liu YT, 2014 Baicalin attenuates brain edema in a rat model of intracerebral hemorrhage. Inflammation 37, 107–115. [PubMed: 23974988]

Zou C, Luo Q, Qin J, Shi Y, Yang L, Ju B, Song G, 2013 Osteopontin promotes mesenchymal stem cell migration and lessens cell stiffness via integrin beta1, FAK, and ERK pathways. Cell Biochem. Biophys 65, 455–462. [PubMed: 23086356]

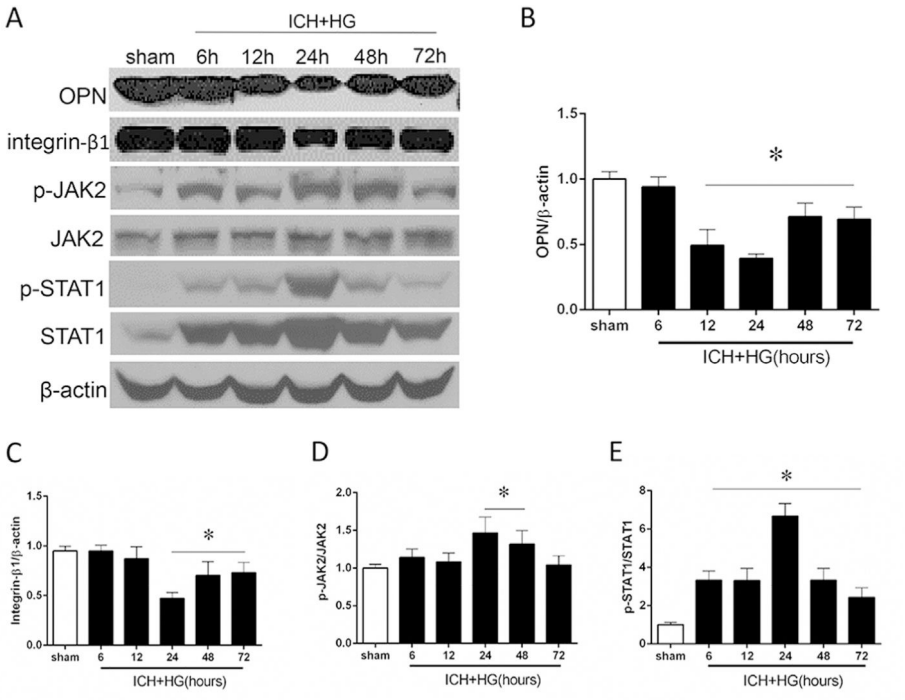

Fig. 1. Time dependent expression changes of OPN and downstream proteins after hyperglycemic intracerebral hemorrhage (ICH + HG).

(A) Representative western blot image and (B) quantitative analyses of the OPN, (C) Integrin-β1, (D) JAK2 and (E) STAT1. n = 6 per group. All data are expressed as mean ± SEM. **P* < 0.05 vs. sham.

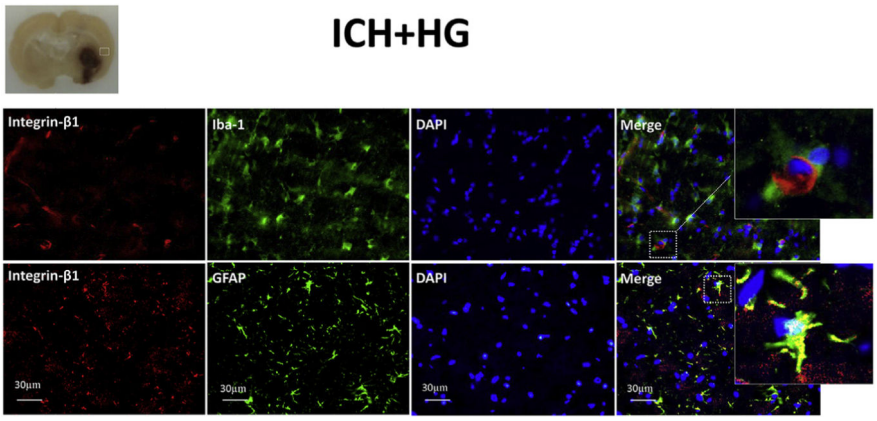

Fig. 2. Colocalization of integrin-β1 in the migroglia (Iba-1) and astrocytes (GFAP) 24 h after hyperglycemic intracerebral hemorrhage (ICH + HG).

Nuclei are stained with DAPI (blue). Top panel indicates the location of staining (small white box) in the brain. Dashed white box in merge panels indicates the colocalization in a single cell. n = 3 per group. Bar = 30 μm.

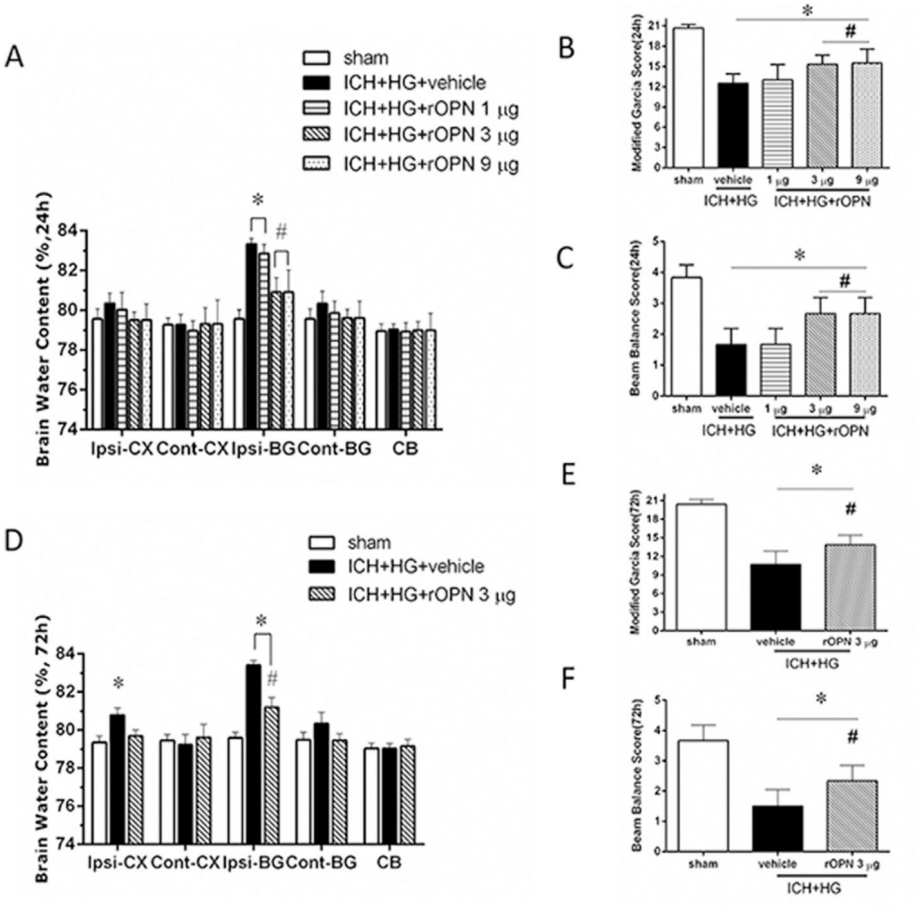

Fig. 3. Intranasal adminstration of recombinant OPN (rOPN) decreased brain edema and improved neurobehavioral function after hyperglycemic intracerebral hemorrhage (ICH + HG).

(A) Brain edema, (B) modified Garcia test and (C) beam balance test 24 h after ICH. (D) Brain edema, (E) modified Garcia test and (F) beam balance test 72 h after ICH. n = 6 per group. Vehicle, sterile 0.9% NaCl; Ipsi, ipsilateral; Cont, contralateral; CX, cortex; BG, basal ganglia; CB, cerebellum; All data are expressed as mean ± SEM, a value of $P < 0.05$ represents statistical significance. *$P < 0.05$ vs. sham; #$P < 0.05$ vs. vehicle treated ICH animals.

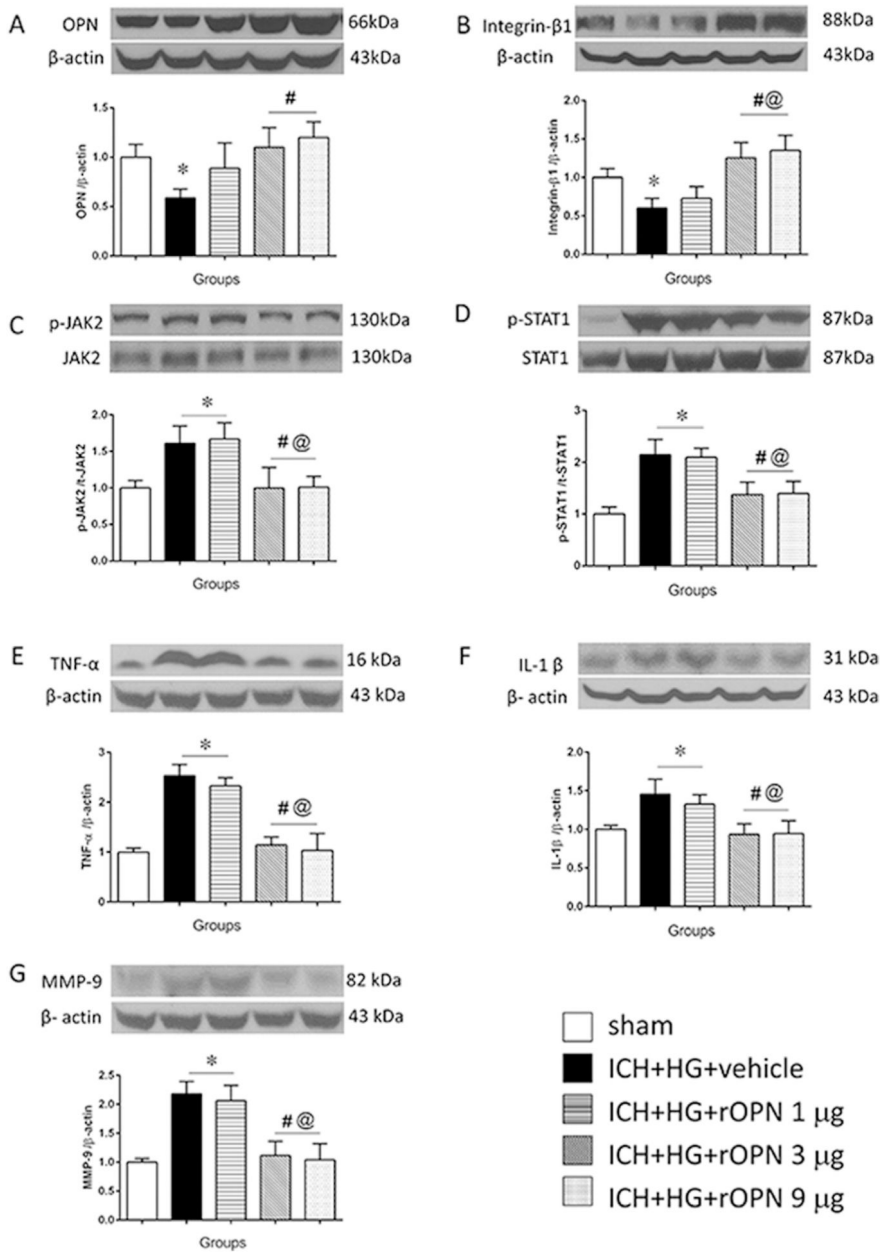

Fig. 4. Effects of recombinant OPN intranasal administration on integrin-β1 expression and JAK2/STAT1 pathway after hyperglycemic intracerebral hemorrhage (ICH + HG).

Representative western blot image and quantitative analyses of the (A) OPN, (B) integrin-β1, (C) JAK2, (D) STAT1, (E) TNF-α, (F) IL-1β (G) MMP-9. n = 6 per group. All data are expressed as mean ± SEM, a value of $p < 0.05$ represents statistical significance. *$P < 0.05$ vs. sham, #$P < 0.05$ vs. sham, #$P < 0.05$ vs. ICH + HG, @ $P < 0.05$ vs. ICH + HG + rOPN 1 μg.

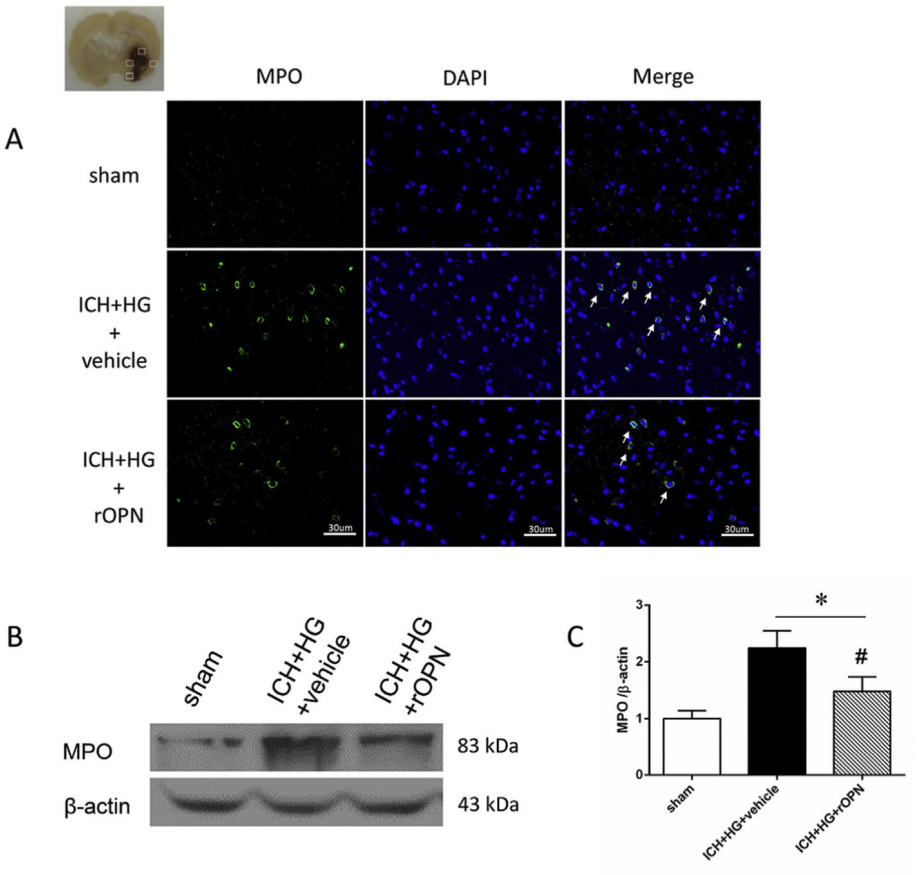

Fig. 5. rOPN decreased ICH + HG induced brain infiltration by neutrophils.

A. No positive cells was found in brain of sham operated animals. ICH + HG increased number of MPO positive neutrophils (green) in brain 24 h after ICH. rOPN attenuated ICH + HG induced brain infiltration by MPO positive neutrophils. Nuclei are stained with DAPI (blue). n = 3 per group. ICH + HG induced significant accumulation of neutrophil marker MPO (B-C). rOPN attenuated ICH induced MPO accumulation. n = 6 per group. $*P < 0.05$ vs. sham, $\#P < 0.05$ vs. ICH + HG + vehicle. (For interpretation of the references to colour in this figure legend, the reader is referred to the Web version of this article.)

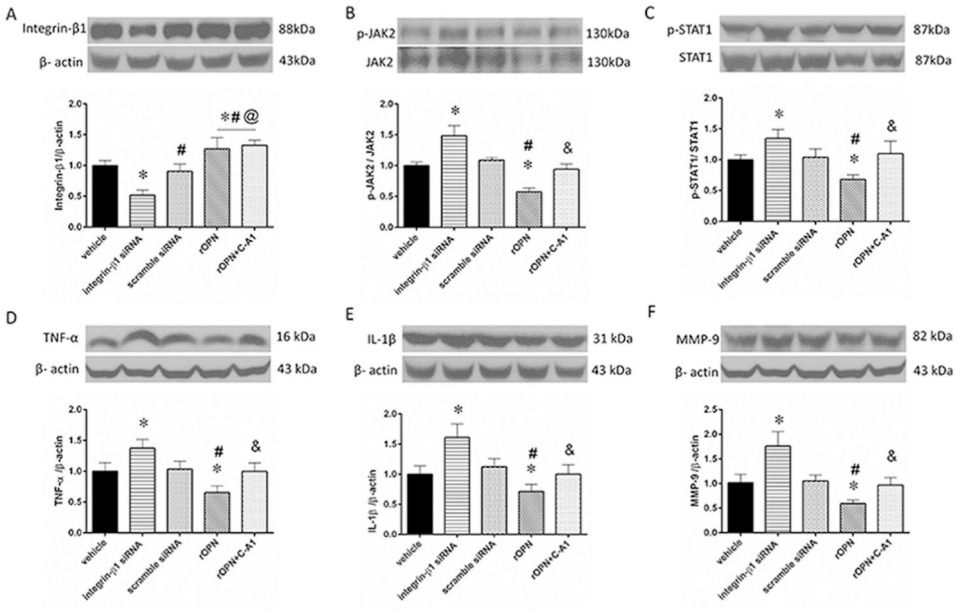

Fig. 6. Effects of Integrin-β1 siRNA and Coumermycin A1(C-A1) on the JAK2/STAT1 pathway of brain inflammation after hyperglycemic intracerebral hemorrhage (ICH + HG).

Representative western blot image and quantitative analyses of the (A) integrin-β1, (B) JAK2, (C) STAT1, (D) TNF-α, (E) IL-1β and (F) MMP-9. n = 6 per group. All data areexpressed as mean ± SEM, a value of $P < 0.05$ represents statistical significance. *$P <$ 0.05 vs. vehicle, *vs. vehicle, #$P < 0.05$ vs. integrin-β1 siRNA, @$P < 0.05$ vs. scramble siRNA, &$P < 0.05$ vs. rOPN 3μg. rOPN, recombinant osteopontin.

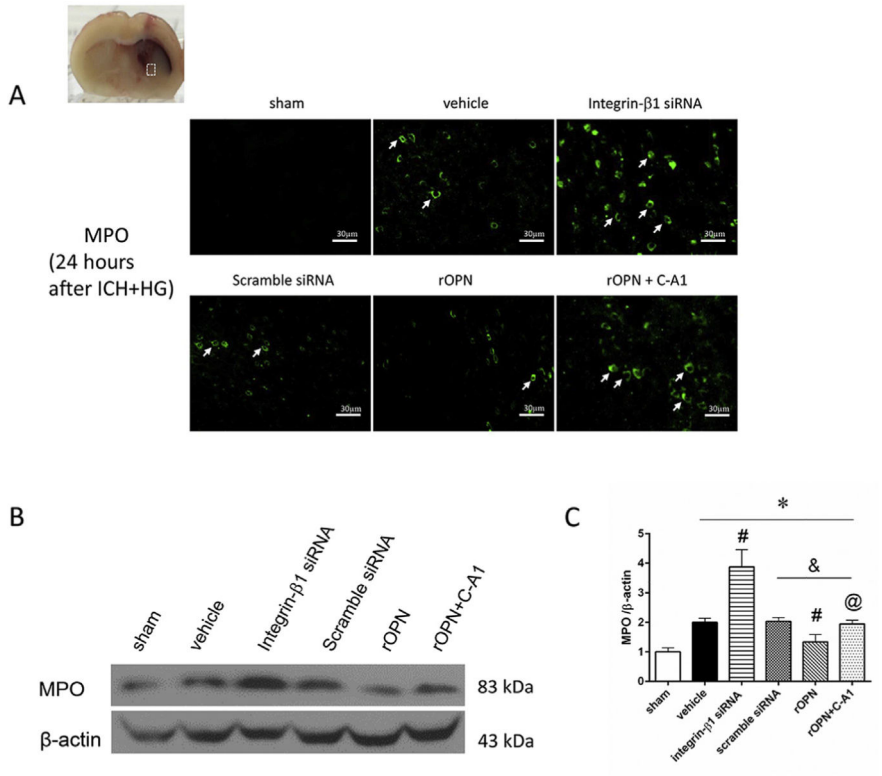

Fig. 7. Intranasal administration of recombinant osteopontin (rOPN) decreased neutrophil infiltration after hyperglycemic intracerebral hemorrhage (ICH + HG).

ICH + HG significantly increased number of MPO positive neutrophils (green A) (n = 3 per group), and accumulation of MPO (**B-C**) (n = 6 per group). While scramble siRNA had no effect, in vivo knock down of integrin-β1 (siRNA) aggravated ICH + HG induced brain infiltration by neutrophils. Intranasal administration of rOPN 3 μg resulted in a decreased number of neutrophils in the brain. C-A1, Coumermycin A1 (**A-C**). All data are expressed as mean ± SEM, a value of $p < 0.05$ represents statistical significance. *$P < 0.05$ vs. sham, #$P < 0.05$ vs. vehicle, & $P < 0.05$ vs. Integrin-β1 siRNA, @ $P < 0.05$ vs. rOPN (For interpretation of the references to colour in this figure legend, the reader is referred to the Web version of this article.)

Table 1

Experimental design and animal numbers used per group. None of sham operated animals died in this study. Average mortality was 8.8% in the experimental animals. No significant difference between treated and untreated subgroups was observed in the mortality. BWC, brain water content; IHC, immunohistochemistry; MPO, myeloperoxidase; ICH + HG, hyperglycemic intracerebral hemorrhage; Vehicle, 0.9% sterile NaCl; siRNA, small interfering ribonucleic acid; Coumermycin A1, an agonist of JAK2.

Groups	Neuro test BWC		Western blot	IHC MPO	Mortality		Sum
	24 h	72 h			24 h	72 h	
Time course study (n = 6; 9 per group): Sham	–		6	3	–		9
ICH + HG (6, 12, 24, 48, 72 h)	–		30 (5)	3	5 (13%)		38
Outcome and Mechanism study:							
Sham	6	6	–	–	–	–	12 (6 + 6)
ICH + HG + Vehicle	6 (1)	6 (2)	6 (1)	3	2 (12%)	2 (25%)	25 (17 + 8)
ICH + HG + rOPN	18 (1)	6 (1)	6	3	1 (4%)	1 (14%)	35 (28 + 7)
ICH + HG + Scramble siRNA			6	3	–		9
ICH + HG + Integrin-β1 siRNA			6	3	–		9
ICH + HG + rOPN + Coumermycin A1			6 (1)	3 (1)	2 (18%)		11
Total	30	18	66	21	13 (8.8%)		148